**International Journal of Advanced Engineering and Technology Research**
ISSN: 3106-8677 (Print), ISSN: 3106-8685 (Online) | Vol. 2, No. 2, 2026

# Research on Key Technologies for Converted-Wave Seismic Data Processing

**Chenghao Jia [1], Hai Su [1, *], Hang Qian [1], Zhongdong Du [2]**

[1] School of Earth Science and Engineering, Xi'an Shiyou Univercity, Xi'an 710065, China

[2] Changqing Geophysical Department, BGP Inc, CNPC, Xi'an 710021, China

[*] **Corresponding author**: (Email: suhai@xsyu.edu.cn)

**Abstract:** Compared with the processing technology of P-wave seismic data, there are still many challenges in the processing of converted-wave seismic data: The initial arrival of the conversion wave cannot be effectively and accurately picked up, and due to the difficulty in establishing an accurate near-surface model of the transverse wave, the calculation of the static correction amount of the conversion wave is difficult, The conventional conversion wave velocity analysis method relies on the establishment of the longitudinal wave velocity model, which is inefficient, Meanwhile, its accuracy is doubly affected by the longitudinal wave velocity and the transverse wave velocity. The conversion wave velocity has multiple solutions, which affects the imaging effect of seismic data.in the light of of the problems above, This paper proposes the multi-information fusion conversion wave static correction technology, the integrated Offset velocity modeling, and the OVT domain (Offset Vector Tile)VTI(Vertical Transverse Isotropy) prestack time offset technology, Through the processing of actual data: The static correction quantity calculated by variable coefficient static correction has higher accuracy than that calculated by constant coefficient static correction, Regularization processing in the OVT domain can effectively reduce the acquisition footprints of the conversion wave data and restore the missing areas of the data, making the amplitude distribution more uniform, Integrated velocity modeling can achieve the interactive update of the four parameters of the conversion wave, effectively improving the processing efficiency and accuracy of the pre-stack time offset of the conversion wave.

**Keywords:** Converted wave, Static correction, OVT domain, VTI media, pre-stack time migration.

## 1. Introduction

With the increasing demands of oil and gas exploration and development companies for exploration targets, the accurate description of the medium properties and spatial distribution characteristics of oil and gas reservoirs has become particularly important. Multi-wave and multi-component seismic exploration, as a key technology in the field of geophysical exploration, utilizes multiple types of information including P-waves, S-waves, and converted waves to conduct detailed investigations of oil and gas reservoirs. Compared with pure P-wave exploration, multi-component seismic exploration can simultaneously obtain P-wave and converted S-wave data, which contain not only subsurface structural information but also anisotropic information such as fractures and fluid properties [1]. This enables better structural imaging, lithology and physical property characterization, and hydrocarbon potential prediction. S-waves mainly reflect the information of rock skeletons, and the S-wave impedance difference between sandstone and mudstone is stable, giving them obvious advantages in sand body identification. P-waves are sensitive to fluids, and the joint analysis and interpretation of P- and S-waves can improve the accuracy and reliability of reservoir and gas-bearing prediction.

Multi-wave and multi-component exploration technology originated in the 1970s, with breakthroughs in technologies such as multiple coverage, vibrator sources, and digital seismology [2]. In the 1990s, with the emergence of Ocean Bottom Node (OBN) seismic exploration technology, onshore multi-wave and multi-component exploration technology began to be explored in China but did not achieve significant results. In the early 21st century, marine multi-wave and multi-component exploration was successfully applied in the Alba Oilfield in the North Sea, UK, and onshore multi-wave and multi-component exploration technology made breakthroughs with the widespread application of three-component digital geophones [3]. In the 2010s, marine multi-wave and multi-component exploration technology continued to develop, and the performance of OBN equipment was significantly improved [4]. Onshore multi-wave and multi-component exploration technology began to be tackled by multiple institutions such as the Southwest Oil and Gas Field and Changqing Oilfield. In the 2020s, marine multi-wave and multi-component exploration technology has continuously integrated advanced technologies such as artificial intelligence and cloud computing, and onshore multi-wave and multi-component exploration technology has made breakthroughs in the tight gas field of the Sichuan Basin [5] and has been widely applied in the exploration of carbonate reservoirs in southern Sichuan [6]. Pan Hui et al. integrated multi-wave component exploration with reservoir P- and S-wave information and proposed a multi-attribute fusion technology, which made reservoir identification more accurate [7].

After decades of exploration of multi-wave and multi-component seismic exploration technology at home and abroad, especially with continuous research in recent years, breakthroughs have been made in the core technologies of multi-wave and multi-component processing and interpretation, and supporting technologies have been gradually improved, showing great application potential.

The key to multi-wave and multi-component seismic data processing lies in converted-wave processing technology. Unlike the mature P-wave seismic data processing technology, converted-wave seismic data processing has long been a

difficult problem [8], especially for seismic data processing in anisotropic media. Scholars and experts such as Tu Shijie, Shi Jianxin, Liu Junfeng, Zhang Liyan, Ren Junsheng, and Zheng Hong have conducted a series of studies [9-14]. However, the calculation of converted-wave static corrections is challenging because both the tomographic inversion method [15] and the refraction method result in low signal-to-noise ratio (SNR) of converted-wave first arrivals after static correction, and it is difficult to pick up first arrivals in complex exploration areas [16]. Converted waves are characterized by asymmetric propagation paths, sensitivity to anisotropic media, and low data SNR, making their imaging far more difficult than that of P-waves [17]. For the above reasons, this paper proposes multi-information fusion static correction and integrated velocity modeling technologies combined with OVT domain VTI prestack time migration technology to solve the core problems of converted-wave processing and achieve more efficient multi-wave and multi-component seismic data processing.

# 2. Principles of Converted-Wave Static Correction and Imaging Methods

## 2.1. Multi-information Fusion Converted-Wave Static Correction

A shear-wave near-surface velocity model is established using high-density microtremor survey points, and the data are constrained by the P-to-S wave velocity ratio obtained from high-precision three-component shear-wave micro-logging [18] to dynamically adjust the static corrections. This overcomes the errors caused by the constant velocity parameter assumption in the constant-coefficient method. The calculation process is as follows:

(1) Construction of shear-wave near-surface velocity model. By densely deploying microtremor survey points, high-frequency reflected signals of near-surface shear waves are collected to obtain the spatial variation characteristics of the shallow shear-wave velocity field $V_S(x, y)$. Three-component shear-wave micro-logging is deployed in key areas to obtain the P-to-S wave velocity ratio $\gamma(x, y)$, which is used to calibrate the microtremor survey data.

(2) Calculation of spatially varying coefficient static correction. Based on the vertical thickness difference $\Delta h(x, y)$ between the surface and the datum, shear-wave velocity, and velocity ratio, the spatially varying static corrections are calculated point by point. The formula is as follows:

$$\Delta T(x,y)=\frac{\Delta h(x,y)[\gamma(x,y)-1]}{\gamma(x,y)\cdot V_s(x,y)} \tag{1}$$

Where $\Delta T(x, y)$ is the long-wavelength static correction of the converted wave at position(x, y), and $\Delta h(x, y)$ is the vertical thickness difference between the surface and the datum at position (x, y), calculated from elevation measurement data.

(3) Three-step optimization correction. On the basis of variable-coefficient tomographic static correction, common-receiver stacking is performed on seismic data to enhance effective signals and suppress random noise, forming high-SNR reference gathers. Then, structure-constrained common-receiver static correction is applied. To eliminate the high-frequency residual time differences not fully corrected in the first two steps and further improve the continuity of events, surface-consistent residual static correction is performed. Finally, the imaging effect is enhanced by a non-global optimization method.

## 2.2. Principles of OVT Domain VTI Prestack Time Migration Imaging

During multi-wave seismic data acquisition, limited by the distribution of shot and receiver points, topographic obstacles and other factors, the data are unevenly distributed in the offset-azimuth domain (OVT domain), leading to acquisition footprints in migration profiles. OVT domain regularization fills data gaps and optimizes gather distribution, improving the stability and accuracy of subsequent migration imaging. On this basis, combined with integrated migration velocity modeling, the efficiency of converted-wave prestack time migration processing is improved. Moreover, actual formations are mostly complex, and traditional isotropic migration algorithms cause position deviations in converted-wave imaging. VTI prestack time migration can solve this problem through anisotropic parameter modeling and algorithm optimization. The specific steps are as follows:

(1) OVT domain bin division of raw seismic data. The bin division formula for PP waves is:

$$\begin{aligned} C_x &= 2\Delta S \\ C_y &= 2\Delta R \end{aligned} \tag{2}$$

The bin division formula for PS waves is:

$$\begin{aligned} C_x &= (\frac{1+\gamma}{\gamma})\Delta S \\ C_y &= (1+\gamma)\Delta R \end{aligned} \tag{3}$$

Where $C_x$ and $C_y$ are the horizontal and vertical bin sizes, respectively; $\Delta S$ is the shot point spacing; $\Delta R$ is the receiver spacing; and $\gamma$ is the P-to-S wave velocity ratio. The reflection point of PP waves is at the midpoint, so the bin size is directly twice the shot and receiver spacing. For PS waves, the reflection point deviates from the midpoint, and the bin size needs to be adjusted according to the velocity ratio $\gamma$. Horizontally, the slower shear-wave velocity causes the reflection point to shift toward the shot point, so the horizontal bin needs to be reduced (the denominator $\gamma$ plays a compression role). Vertically, the faster P-wave velocity results in shorter reflection time, so the vertical bin needs to be enlarged (the coefficient $1+\gamma$ plays a stretching role).

(2) OVT domain data regularization. Due to the uneven distribution of acquired data, interpolation is required to fill empty bins. The Inverse Distance Weighting (IDW) interpolation method is used, with the formula:

$$Z(x_0)=\frac{\sum_{i=1}^{N}\frac{Z_i}{d_i^p}}{\sum_{i=1}^{N}\frac{1}{d_i^p}} \tag{4}$$

Where $Z(x0)$ is the estimated value of the point to be interpolated x0; Zi is the observed value of the known point xi; di is the distance from the known point xi to the point to be interpolated x0; p is the power exponent, usually taken as 2; and N is the number of known points involved in interpolation. The value of an unknown point is estimated by distance weights, where the weight of a known point is

inversely proportional to its distance from the unknown point—the closer the distance, the greater the weight.

(3) Integrated migration velocity modeling. Converted waves have asymmetric propagation paths, and their time-distance equation is a double square root equation [19], with multiple imaging parameters. To improve the efficiency and accuracy of converted-wave velocity modeling, this paper proposes an integrated migration velocity modeling technology, which integrates P-wave and converted-wave data to jointly optimize key parameters in the velocity model and construct a unified velocity model. The converted-wave traveltime equation in VTI media is [20]:

$$t_c = \sqrt{\frac{t_{co}}{1+\gamma_0} + \frac{(x+h)^2}{v_{fz}^2} - 2\eta_e \Delta t_p^2} + \sqrt{(\frac{\gamma_0 t_{co}}{1+\gamma_0})^2 + \frac{(x-h)^2}{v_{sz}} + 2\xi_e \Delta t_s^2} \quad (5)$$

Where $t_c$ is the converted-wave traveltime; x is the offset; $t_{co}$ is the converted-wave vertical two-way traveltime; h is the half offset; $v_{fz}$ and $v_{sz}$ are the P-wave and S-wave velocities, respectively; $\gamma_0$ is the average P-to-S wave velocity ratio; $\eta_e$ and $\eta_e$ are the anisotropic parameters of P-waves and S-waves, respectively; and $\Delta t_p^2$ and $\Delta t_s^2$ are the normal moveout (NMO) terms, with their equations:

$$\Delta t_p^2 = \frac{(x+h)^4}{v_{fz}^2\left[\frac{t_{co}^2 v_{fz}^2}{(1+\gamma_0)^2} + (1+2\eta_e)(x+h)^2\right]} \quad (6)$$

$$\Delta t_s^2 = \frac{(x-h)^4}{v_{sz}^2\left[\frac{t_{co}^2 v_{sz}^2 \gamma_0^2}{(1+\gamma_0)^2} + (x-h)^2\right]} \quad (7)$$

The four parameters for converted-wave prestack time migration are the converted-wave NMO velocity $v_{c2}$, average P-to-S wave velocity ratio $\gamma_0$, equivalent P-to-S wave velocity ratio $\gamma_e$, and anisotropic parameter $\chi$. The relationships between these parameters are as follows:

$$v_{fz}^2 = v_{c2}^2 \frac{\gamma_e(1+\gamma_0)}{1+\gamma_e} \quad (8)$$

$$v_{sz}^2 = v_{c2}^2 \frac{1+\gamma_0}{\gamma_0(1+\gamma_e)} \quad (9)$$

$$\eta_e = \frac{\chi_e}{(\gamma_0 - 1)\gamma_e^2} \quad (10)$$

$$\xi_e = \frac{\chi_e}{\gamma_0 - 1} \quad (11)$$

First, each parameter is initialized: the initial P-wave velocity vp is obtained by tomographic inversion, the initial $v_{c2}$ is derived from empirical formulas, the initial $\gamma_0$ takes the regional value, and the initial values of $\eta_e$ and $\xi_e$ are set according to the prior geological model. Then, the four parameters are jointly optimized: the small-offset converted-wave data are subjected to hyperbolic NMO to optimize $v_{c2}$ and flatten the near-offset events; the medium-offset data of P-waves and converted waves are used to invert $\gamma_0$ and $\gamma_e$ to align the P-wave and converted-wave events; finally, based on the iteratively updated $\gamma_0$ and $\gamma_e$, the anisotropic parameters $\eta e$ and $\xi_e$ are updated through anisotropic NMO of large-offset converted-wave data.

(4) Migration imaging is performed using the converted-wave traveltime equation in VTI media (Equation 5) with the four converted-wave parameters determined by multi-wave integrated migration velocity modeling.

# 3. Converted-Wave Static Correction

Figure 1c shows the converted-wave stack profile obtained after spatially varying coefficient static correction. Comparing with the converted-wave profiles obtained by elevation static correction (Figure 1a) and constant-coefficient static correction (Figure 1b), it can be seen that the stack profile obtained by the method proposed in this paper has more continuous and clear events, realizing the transformation from low-precision constant-coefficient to high-precision variable-coefficient converted-wave static correction with obvious application effects.

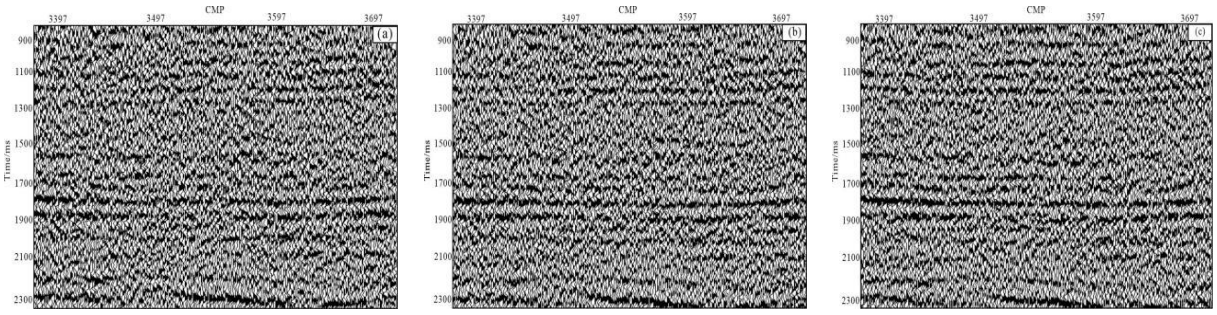


(a) Height statics; (b) P-wave surface correction *2.0; (c) Space variable ratio * P wave surface correction

**Figure 1.** Each static correction converted wave superposition profile

On the basis of spatially varying coefficient static correction, other static correction techniques are further applied to improve imaging accuracy. Figure 2(a) is obtained by applying variable-coefficient tomographic static correction. On this basis, common-receiver stacking is performed, and residual time differences are counted in common-receiver gathers to eliminate medium- and short-wavelength errors. Figure 2(b) is obtained after structure-constrained common-receiver static correction for converted waves. Then, high-frequency residuals are iteratively optimized, and surface-consistent residual static correction and nonlinear global optimization are performed to obtain Figure 2(c). The comparison shows that after the three-step static correction, the imaging effect of the shallow and middle

layers in the converted-wave stack profile is significantly improved, which is of great help to subsequent processing work.

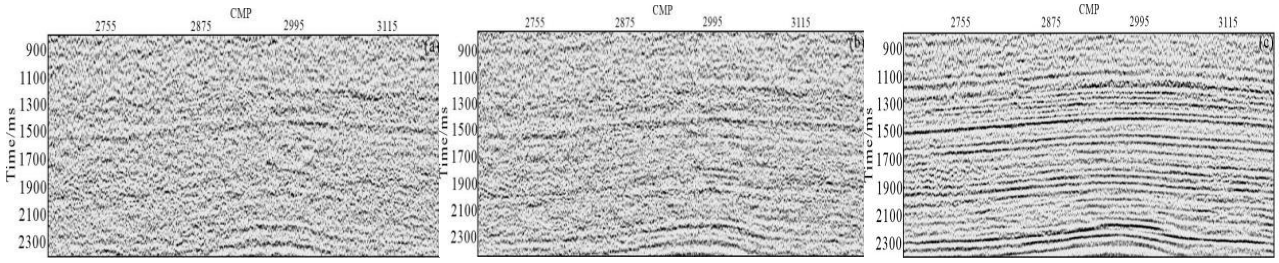


(a) Variable coefficient statics converted wave stack profile; (b) Common-detector statics converted wave stack profile; (c) Residual statics converted wave stack profile

**Figue 2.** Three-step optimization of statics converted wave stack profile

# 4. Converted-Wave Prestack Time Migration Imaging

Figure 3(a) shows the OVT domain bin distribution before regularization, which presents alternating sparse and dense areas with blank regions. After regularization, the bin distribution (Figure 3b) tends to be continuous and uniform, and the blank areas are filled. Figure 4(a) is the amplitude slice of converted waves before regularization, which shows obvious acquisition footprints, uneven amplitude distribution, and local data missing. The regularized amplitude slice (Figure 4b) has significantly reduced noise, filled data gaps, and more uniform amplitude distribution.

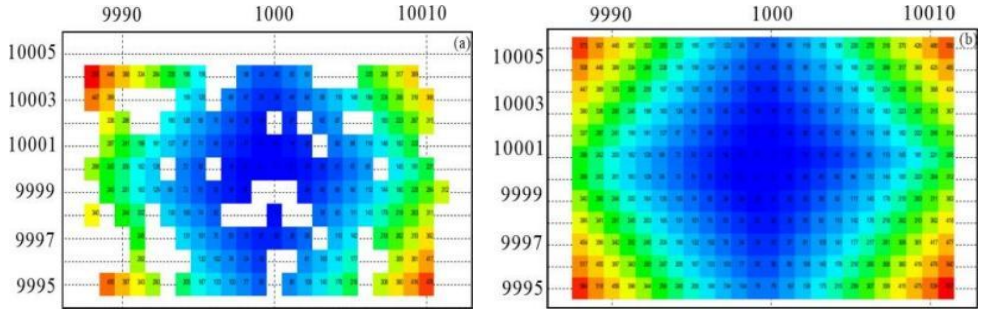


(a) Surface element distribution in OVT domain before regularization; (b) Surface element distribution in OVT domain after regularization

**Figure 3.** Surface element distribution in OVT domain before and after conversion wave regularization

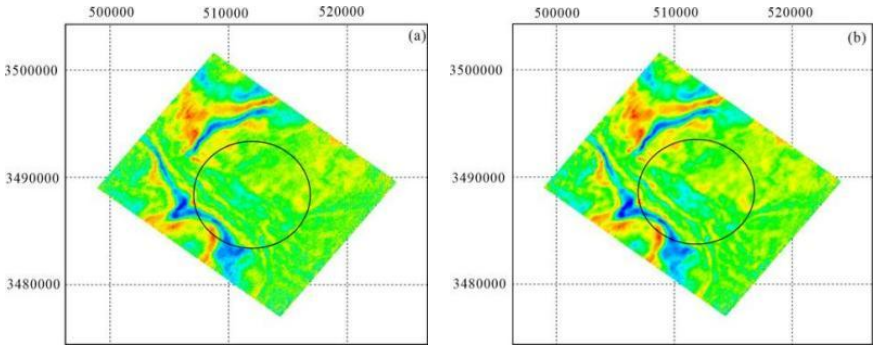


(a) Pre-regularization amplitude slice (3500ms); (b) Regularized amplitude slice (3500ms)

**Figure 4.** OVT domain amplitude slices before and after conversion wave regularization

Using the multi-wave integrated migration velocity modeling technology, joint $\gamma_0$ picking and interactive $\gamma_e$ updating for P-waves and converted waves are realized, replacing the waiting problem for P-wave velocity fields. The processing efficiency of converted-wave prestack time migration is improved by more than 30%, greatly accelerating the submission of converted-wave processing results (Figure 5).

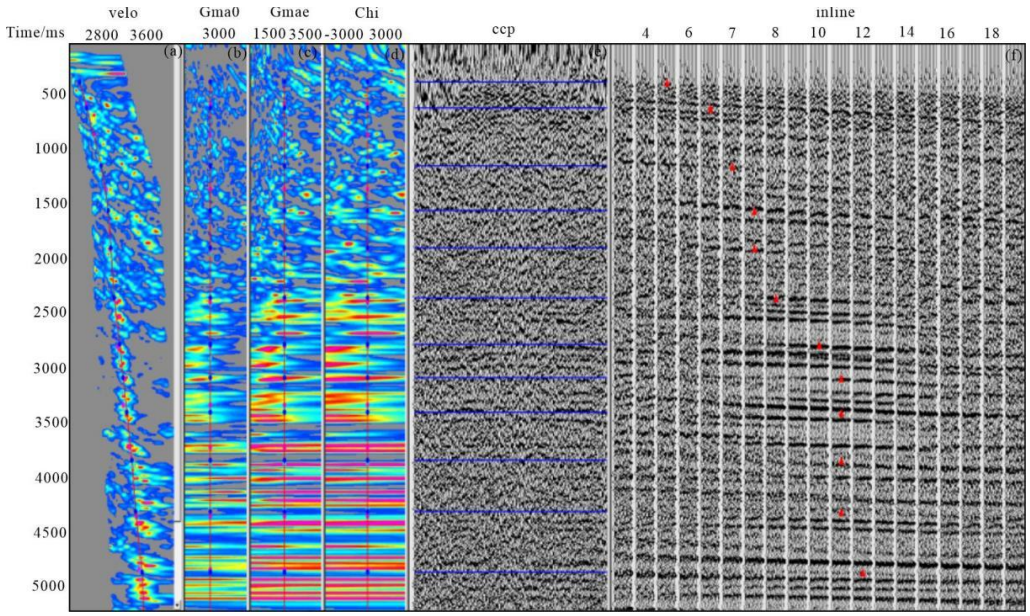


(a) $v_{c2}$ spectrum; (b) $\gamma_0$ spectrum; (c) $\gamma_e$ spectrum; (d)$\chi$ spectrum; (e)ccp gather; (f)cmp gather

**Figure 5.** Conversion wave four-parameter analysis interactive picking

Figure 6 shows the migration gathers before and after VTI anisotropy correction for converted waves in the OVT domain. The comparison shows that after anisotropy correction, the SNR of converted-wave migration gathers is significantly improved, the continuity of reflection events is enhanced, and the gather flattening effect is obviously improved. This indicates that the velocity model after anisotropy correction is more accurate, providing a reliable basis for subsequent imaging processing.

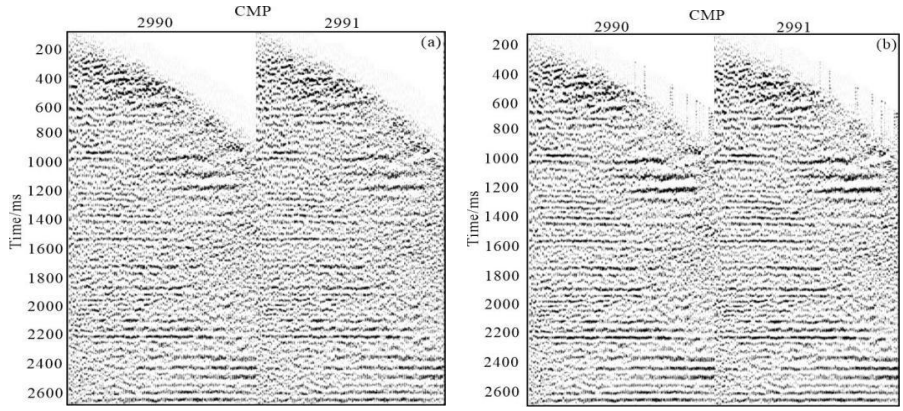


(a) Before conversion wave anisotropy correction; (b) Converted wave anisotropy corrected

**Figure 6.** OVT domain offset track set before and after conversion wave anisotropy correction

Figure 7a is the conventional converted-wave prestack time migration profile. Comparing with the OVT domain anisotropic prestack time migration profile of converted waves (Figure 7b), it can be seen that the migration profile obtained by the method used in this paper has better event continuity and higher imaging accuracy, which is more conducive to subsequent lithologic body characterization and interpretation.

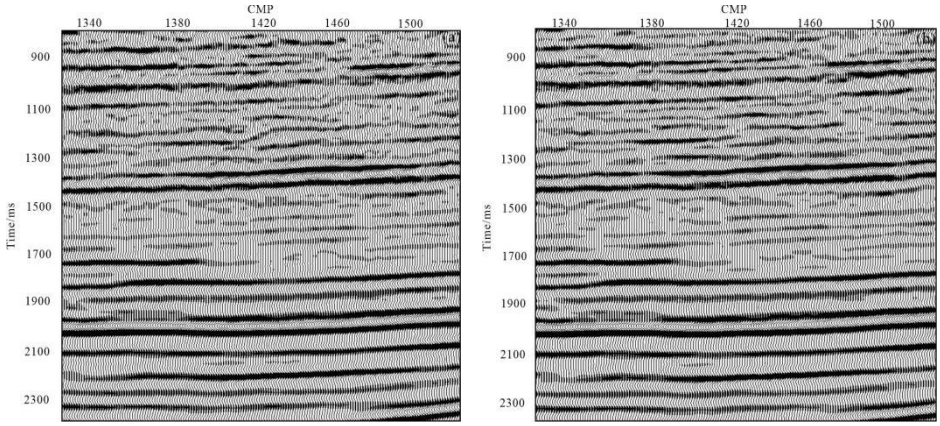


(a) Converted wave conventional prestack time migration profile; (b) Converted wave OVT domain anisotropic prestack time migration profile

**Figure 7.** Converted wave OVT domain anisotropy pre-stack time migration profile

# 5. Conclusions

In the process of processing field converted-wave data in complex areas, aiming at the problems of difficult converted-wave static correction, low efficiency of fine velocity modeling, and poor imaging effect, this paper proposes multi-information fusion static correction technology and OVT domain VTI prestack time migration technology (combined with integrated velocity modeling technology) to process converted-wave data. The following conclusions are drawn:

(1) The multi-information fusion converted-wave static correction technology can effectively calculate accurate converted-wave static corrections, realizing the transformation from low-precision constant-coefficient to high-precision variable-coefficient static correction processing.

(2) The application of OVT domain regularization processing technology in converted-wave velocity modeling can effectively reduce acquisition footprints, fill data gaps, and make the amplitude distribution more uniform.

(3) The integrated migration velocity modeling technology enables interactive updating of four converted-wave parameters, effectively improving the efficiency and accuracy of converted-wave prestack time migration processing.

# Acknowledgment

Graduate Innovation and Practical Ability Training Program of Xi'an Shiyou University (No. YCS23213066)

Biography: Jia Chenghao (2002–), male, born in Jingmen, Hubei Province, Master candidate, mainly engaged in seismic signal processing technology.

# References

[1] Lu, J., Wang, Y., Ji, Y. X., et al. (2018). Imaging technology for multi-component seismic data. Chinese Journal of Geophysics, 61(8), 3499–3514.

[2] Gruszczyk, E., Trzesnioswki, Z., & Misiaczek, P. (2003). Chalupki Debnianskie Field: Improving drilling success in shallow gas reservoirs with VectorSeis. First Break, 21(2), 37–43.

[3] Wu, S. K., Zhou, M. F., Shen, W. J., et al. (2004). Application of three-component seismic exploration technology with digital geophones. Oil Geophysical Prospecting, 39(6), 602–604, 14.

[4] Alerini, M., Traub, B., Ravaut, C., et al. (2009). Prestack depth imaging of ocean-bottom node data. Geophysics, 74(6), WCA57–WCA63. https://doi.org/10.1190/1.3238359

[5] Yang, W., Yang, Z., Wang, X. W., et al. (2022). Multi-wave joint denoising method and its application in tight gas in central Sichuan. Oil Geophysical Prospecting, 57(S2), 16–22, 223–224.

[6] Xie, W. X., Mei, A. X., Chen, D., et al. (2026). Application and effect of converted-wave seismic imaging technology in carbonate reservoir exploration in southern Sichuan. Progress in Geophysics, 41(1), 341–354.

[7] Pan, H., Gao, J. H., Gui, J. Y., et al. (2024). A multi-scale attribute fusion method based on multi-wave seismic data. Oil Geophysical Prospecting, 59(4), 856–864.

[8] Qian, Z. P., Sun, P. Y., Xiong, D. Y., et al. (2023). Research and application of converted-wave static correction method for complex structures. Oil Geophysical Prospecting, 58(2), 325–333.

[9] Tu, S. J., Pang, Q. K., Wang, L., et al. (2006). Converted-wave data processing and fracture prediction in YC area. Progress in Geophysics, 21(2), 512–519.

[10] Shi, J. X., Wang, Y. G., Bi, L. F., et al. (2006). Research on processing and interpretation technology of multi-component seismic data. Progress in Geophysics, 21(2), 505–511.

[11] Liu, J. F., Meng, X. H., Yu, C. L., et al. (2010). Application of 3D converted-wave seismic data processing technology in LMD area. Oil Geophysical Prospecting, 45(1), 99–104, 164, 173.

[12] Zhang, L. Y., Wang, J. M., Li, A., et al. (2011). 3D converted-wave prestack azimuthal anisotropy correction technology. Oil Geophysical Prospecting, 46(5), 695–699, 731, 836, 660.

[13] Ren, J. S., & Shen, X. Z. (2015). Inversion of crustal anisotropic structure based on receiver functions and neighborhood algorithm. Progress in Geophysics, 30(5), 2043–2054.

[14] Zheng, H., Fan, J. K., Li, C. L., et al. (2021). Distribution characteristics of anisotropy, crustal thickness and Poisson's ratio in Shandong area. Progress in Geophysics, 36(5), 1905–1915.

[15] Qin, J. J., Yuan, H. K., He, Y. J., et al. (2018). Application of tomographic imaging technology in urban active fault detection. Progress in Geophysics, 33(5), 2153–2158.

[16] Yang, Z., Wang, X. W., Su, Q., et al. (2020). VTI velocity modeling for converted-wave prestack time migration in complex areas. Oil Geophysical Prospecting, 55(S1), 33–40, 5.

[17] Li, A., Zhang, L. Y., Li, S. C., et al. (2021). Research on 5D interpolation technology in OVT domain based on matching pursuit algorithm. Progress in Geophysics, 36(4), 1541–1546.

[18] Li, G. H., & Zhu, G. M. (2006). Investigation of near-surface P- and S-wave velocities using three-component micro-logging technology. Oil Geophysical Prospecting, 41(2), 160–165, 248, 15–16.

[19] Cui, J., Han, L. G., Lian, Y. G., et al. (2009). High-resolution P-SV wave velocity analysis. Progress in Geophysics, 24(6), 2036–2043.

[20] Dai, H. C., & Li, X. Y. (2007). Velocity model updating in prestack Kirchhoff time migration for PS converted waves: Part I—Application. Geophysical Prospecting, 55(4), 549–559. https://doi.org/10.1111/j.1365-2478.2007.00632.x